Journal of Intelligent and Robotic Systems 7: 195–213, 1993.

Rule-Based Supervisory Control of a Two-Link Flexible Manipulator

ERICK GARCÍA-BENITEZ, STEPHEN YURKOVICH, and KEVIN M. PASSINO★
Department of Electrical Engineering, The Ohio State University, 2015 Neil Avenue, Columbus, OH 43210, U.S.A.

(Received: 19 March 1991; accepted: 20 June 1991)

Abstract. In this paper, we propose a two level hierarchical control strategy to achieve accurate end-point position of a planar two-link flexible manipulator. The upper level consists of a feedforward rule-based supervisory controller that incorporates fuzzy logic, whereas the lower level consists of conventional controllers that combine shaft position-endpoint acceleration feedback for disturbance rejection properties and shaping of the (joint) actuator inputs to minimize the energy transferred to the flexible modes during commanded movements. The effectiveness of this hierarchical control strategy is verified by experimental results for various movements of the links, in various configurations. In particular, we illustrate how the hierarchical intelligent control strategy performs better than conventional control techniques for endpoint position control in the presence of flexure effects.

Key words. Flexible manipulators, fuzzy logic, fuzzy control, hierarchical control.

1. Introduction

In the control of complex dynamical systems conventional control techniques are often unable to achieve the design objectives over a wide range of operating conditions. Such inadequate control performance often results from (i) nonlinear and time-varying plant dynamics, (ii) significant noise and disturbances, and (iii) limitations of control methodologies so that they only apply to neighborhoods of operating points. The objective of 'intelligent control' is to augment conventional control techniques to widen the operating range of the system and achieve demanding design objectives [1, 2]. Here, we introduce a hierarchical intelligent control strategy for a two-link flexible manipulator and show that the proposed hierarchical controller can in fact widen its operating range as compared to conventional controllers.

One way to motivate the use of the rule-based hierarchy would be to provide a complete assessment of current conventional techniques for flexible manipulator control, especially from an experimental viewpoint. This is not our intent here, but the interested reader may wish to pursue the cited references; some of the more recent visible experimental efforts have been the work at Ohio State and Stanford [3–6], among others. While most experimental studies have focused on single-link manipulators, or multi-link manipulators with a single flexible link, such setups have served as valuable testbeds for modeling, system identification and controller design.

★ Corresponding author: phone: (614) 292-5716; email: passino@eagle.eng.ohio-state.edu

Controlling coupled flexible member systems (multilink) remains an open problem, however, particularly from the implementation viewpoint. For this paper we focus our attention on the endpoint position control of a two member system, assuming a fixed reference frame for the base, with two rotary joints. We propose a two level hierarchical control strategy to achieve accurate end-point position, where the upper level consists of a feedforward rule-based supervisory controller that incorporates fuzzy logic for controller parameter selection. The control perspective we adopt for the lower level in the hierarchy is to implement a two-stage, or composite, control strategy in which the vibration control problem for fine motion endpoint positioning is considered separate from the gross motion, large angle skew problem. In the first stage, an input shaping scheme is used to alter the actuator inputs in such a way that minimal energy is injected into the flexible modes [7, 8]. Such methods for slewing control seek to shape the input via convolution with a sequence of impulses, based on the idea that superposition of impulse responses can produce a movement with no vibrational motion after the input has ended.

While [9] represents the first work of its kind in the area of combined input shaping-acceleration feedback for control of flexible manipulators, several shortcomings presented in that study manifest themselves for rapid, large-angle movements. Difficulties arise due to the nature of coupled flexure effects [10]. That is, through large-angle movements the manipulator experiences significant variations in the modal frequencies of the flexible links. Since the shaped inputs to the actuators rely on accurate knowledge of these modal frequencies, the precalculated inputs require *a priori* knowledge of the frequencies based on the commanded movement. Moreover, an inherent relationship exists between the commanded speed of the manipulator movement and endpoint position control performance, thus affecting the choice of gain parameters in the composite control strategy.

The continuous relationship between flexible link modal frequencies and the commanded movement (link angles and speed) has motivated the need for a supervisory level for controller selection (for example, input shaping alone, or composite strategies), for input shaping parameters, and for generation of appropriate reference input profiles. The tool chosen for implementation of this supervisory level is a rule-based fuzzy logic framework. The main contribution of the paper is the development of a novel fuzzy supervisory control approach for an experimental two-link flexible manipulator. Moreover, it is shown how the hierarchical control approach improves the performance of current techniques for endpoint position control in the presence of flexure effects.

2. Problem Overview

The control objective for the two-link manipulator in this study is simply stated: maintain endpoint position in the presence of severe flexure effects, for movements and configurations spanning the entire workspace of the apparatus (the complete operating range).

The apparatus considered in this work consists of two flexible links situated in the horizontal plane. The first link, which is driven by a 3.4 ft-lb direct drive servo-motor is 0.75 m long, 0.127 m high, and is made of 2.3 mm thick aluminum, with a counterweight centered about the motor axis for balance and protection of motor bearings. Mounted at the endpoint of the first link is a geared servomotor to actuate the smaller (0.5 meter long, 0.038 m high) second link made of 1 mm thick aluminium. The joint consists of a free rotating hub set between two bearings, allowing approximately $\pm 170°$ rotation. Both joints have allocated velocity and position sensors.

Lightweight accelerometers (6.7 grams in a 0.56 inch round casing) are mounted at the endpoint of each link for measuring linear acceleration. Additional sensing for data recording only is provided by a linear array line scan camera to record the second link endpoint position. The relatively small field of view of the camera limits its usefulness for large angle motions; for this reason, results are typically displayed for the final phase of the overall motion. More details on the apparatus may be found in [11], [9], and [10].

3. Low Level Control Algorithms

3.1. INPUT SHAPING

Input shaping is an open-loop compensator which shapes the actuator input in such a way that vibrational motion is eliminated after the input has ended [7]. Implementation involves convolving a sequence of impulses with commanded reference inputs. The action of adding an appropriately delayed impulse response to another impulse response is, essentially, to add zeros to the system function at the exact location of the system poles, thus cancelling the effect of these dynamics. To illustrate this point consider a second-order system consisting of a pair of complex poles located in the complex s-plane at $s = -\sigma \pm jw$. Furthermore, assume that $h(t)$ is the system impulse response, and let the system input be a sum of impulses of the form

$$u = \alpha_0 \delta(t) + \alpha_1 \delta(t - t_1). \tag{1}$$

The Laplace representation of the system output, $y(t)$, is given by

$$\begin{aligned} Y(s) &= \alpha_0 H(s) + \alpha_1 \exp^{-st_1} H(s) \\ &= \alpha_1 H(s) \left(\frac{\alpha_0}{\alpha_1} + \exp^{-st_1} \right), \end{aligned} \tag{2}$$

where $H(s)$ is the s-domain representation of $h(t)$. It is evident that the term enclosed in parentheses introduces an infinite number of zeros to the system.

For control purposes it is necessary to determine the parameters of the input, i.e. α_0, α_1, t_1. By setting the fundamental pair of complex zeros introduced in (1) and (2) to zero for a specific value of s,

$$\frac{\alpha_0}{\alpha_1} + \exp^{-st_1} = 0, \tag{3}$$

the poles of $H(s)$ are exactly canceled when

$$\frac{\alpha_0}{\alpha_1} = -\exp^{\sigma t_1}\exp^{\pm j\omega t_1}, \tag{4}$$

where t_1 is the second impulse application time and ω is the damped frequency of the system poles. Equating both imaginary and real parts of the expression above, we obtain

$$-1 = \exp^{\pm j\omega t_1}, \tag{5}$$

$$\frac{\alpha_0}{\alpha_1} = \exp^{\sigma t_1}. \tag{6}$$

Solving for the application time of the second impulse in Equation (5) yields

$$t_1 = \pi/\omega. \tag{7}$$

It is important to note that this form of the expression for t_1 is amenable for control implementation since the modal frequencies can be easily determined either experimentally or via system identification. For example, in this work the modal frequencies of the two-link flexible manipulator for each link may be obtained by analyzing the link endpoint acceleration in the frequency domain through the Fast Fourier transform (FFT), and detecting the peaks of the transformed signal [10,12,13].

The amplitudes of the impulses in Equation (1) can also be determined in terms of the system modal damping ζ by recalling that

$$\omega = \omega_n\sqrt{1-\zeta^2}, \tag{8}$$

$$\zeta = \sigma/\omega_n, \tag{9}$$

where ω_n is the natural undamped frequency of the system. Therefore, Equation (6) can be rewritten as

$$\frac{\alpha_0}{\alpha_1} = \exp\left(\frac{\zeta\pi}{\sqrt{1-\zeta^2}}\right). \tag{10}$$

Imposing the constraint $\alpha_0 + \alpha_1 = 1$ on the impulse amplitudes (to ensure that the shaped input voltage energy has the same energy as the reference voltage) results in

$$\alpha_0 = \frac{1}{1+\exp\left(\dfrac{-\zeta\pi}{\sqrt{1-\zeta^2}}\right)}, \tag{11}$$

$$\alpha_1 = \frac{\exp\left(\dfrac{-\pi\zeta}{\sqrt{1-\zeta^2}}\right)}{1+\exp\left(\dfrac{-\zeta\pi}{\sqrt{1-\zeta^2}}\right)}. \tag{12}$$

It can be noticed from Equations (7), (11) and (12) that the critical parameters (ω and ζ) of the input scheme must be known *a priori* for the algorithm to be implemented. Furthermore, since this is an open loop scheme, it is sensitive to parameter disturbances, although in [7] it is shown that robustness to frequency uncertainty can be increased by adding more impulses to the input sequence, at the obvious expense of introducing more lag to the system.

To shape an input for more than one vibrational mode, the above concept generalizes by designing an impulse for each mode individually. These sequences are then convolved together to form a new impulse sequence which is convolved with the reference input, $r(t)$. For the case of this two-link flexible manipulator two modes of vibration are considered in each link [9], so that the new impulse sequence takes the form

$$\begin{aligned}&[\alpha_0\delta(t) + \alpha_1\delta(t - t_1)] * [\beta_0\delta(t) + \beta_1\delta(t - t_2)]\\ &\quad = \alpha_0\beta_0\delta(t) + \alpha_1\beta_0\delta(t - t_1) + \alpha_0\beta_1\delta(t - t_2) + \alpha_1\beta_1\delta(t - t_1 - t_2), \quad (13)\end{aligned}$$

where $*$ denotes the convolution operation. Both reference inputs are constant voltages with their amplitudes and duration times denoted by A_1, A_2 and t_{01}, t_{02}, respectively.

3.2. COMPOSITE CONTROL

In [9], a decentralized method using shaft position-endpoint acceleration proportional feedback control was demonstrated to be successful in eliminating endpoint vibrations for large angle maneuvers for this manipulator, provided that the control parameters are properly tuned. Link endpoint acceleration data and actuator shaft position data from the two links are subtracted from reference values to form error signals. These error signals are then multiplied by appropriate gains and added together to form control inputs to the two actuators:

$$u_1(k) = K_{p1}(\theta_{\text{ref}1} - \theta_1(k)) - K_{a1}\gamma_1(k), \quad (14)$$

$$u_2(k) = K_{p2}(\theta_{\text{ref}2} - \theta_2(k)) - K_{a2}\gamma_2(k), \quad (15)$$

where $u_i(k)$ are the control inputs, $\theta_{\text{ref}i}$ are the reference motor shaft positions, $\theta_i(k)$ are the measured motor shaft positions, $\gamma_i(k)$ are the measured link endpoint accelerations, and K_{pi}, K_{ai} are the shaft position and endpoint acceleration feedback gains, respectively. The shaft position gains are used to control actuator angular position, while the endpoint acceleration gains are used to introduce damping to the links.

This simple feedback scheme and the input shaping configuration are combined to form the composite controllers shown in Figure 1. In the composite 1 configuration the change from input shaping to shaft position-endpoint acceleration feedback occurs at the end of the convolved input signal, $t = T$; this is denoted in the figure

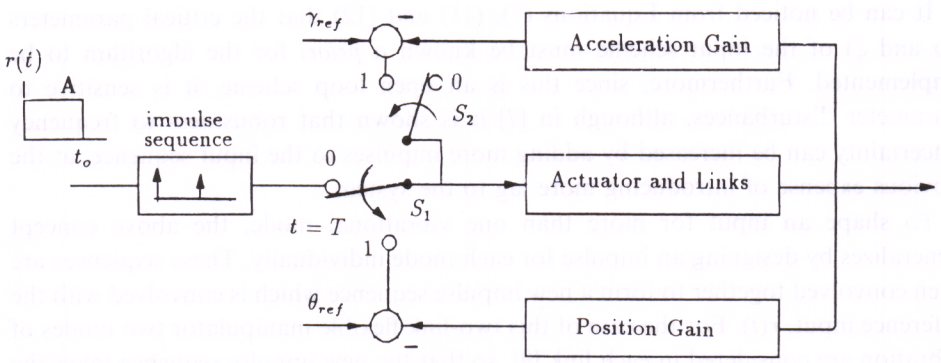

controller number	controller type	switch positions $S_1(t=0)$	$S_1(t>T)$	$S_2(t=0)$	$S_2(t>T)$
1	input shaping	0	0	0	0
2	composite 1	0	1	0	1
3	composite 2	0	1	1	1

Fig. 1. Controller configuration possibilities.

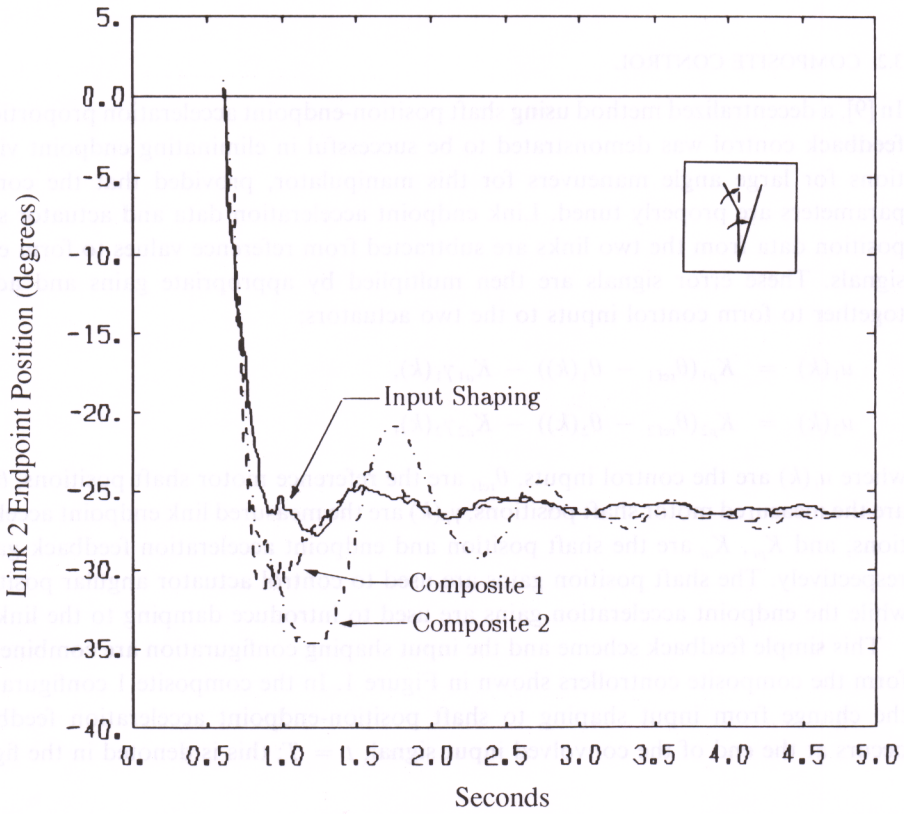

Fig. 2. Link 2 endpoint position for small-combined link slews.

by moving the switches S_1 and S_2 to their 1 positions simultaneously. In the composite 2 configuration the control scheme employs acceleration feedback from the outset (when $t = 0$); the legend in Figure 1 summarizes the switch positions for input shaping alone, composite 1, and composite 2. The motivation for defining three different strategies is to take advantage of the best properties of each for various robot orientations and movements, as well as for various magnitude (large and small angle) slews. This point is illustrated next.

3.3. PERFORMANCE EVALUATION

In this section, the performance of each of the controller types is examined for three different link slews; small angle-combined movement, large angle-combined movement (combined movement refers to the links moving in the same direction) and large angle-counter relative movement (links moving in opposite directions). Link 2 endpoint position in all of the plots presented in this paper is read by the linear array camera, where the angular position on the vertical axis (in degrees) has no significance since it is relative only to the end of the maneuver. Figure 2 shows link 2 endpoint

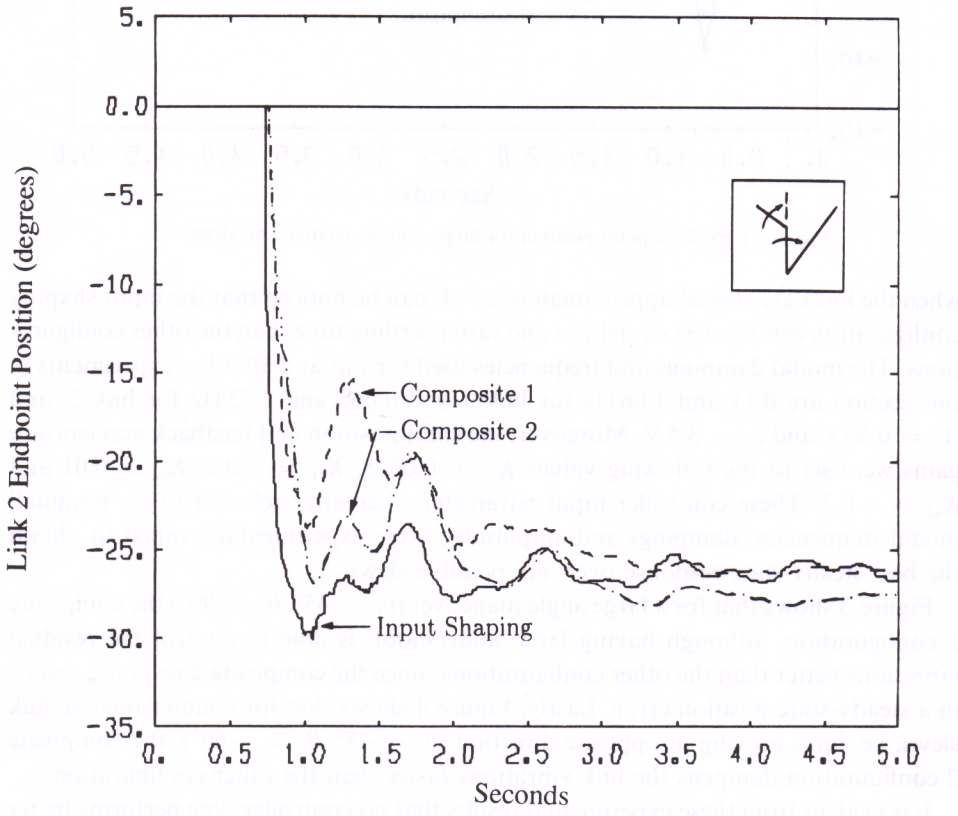

Fig. 3. Link 2 endpoint position for large-combined link slews.

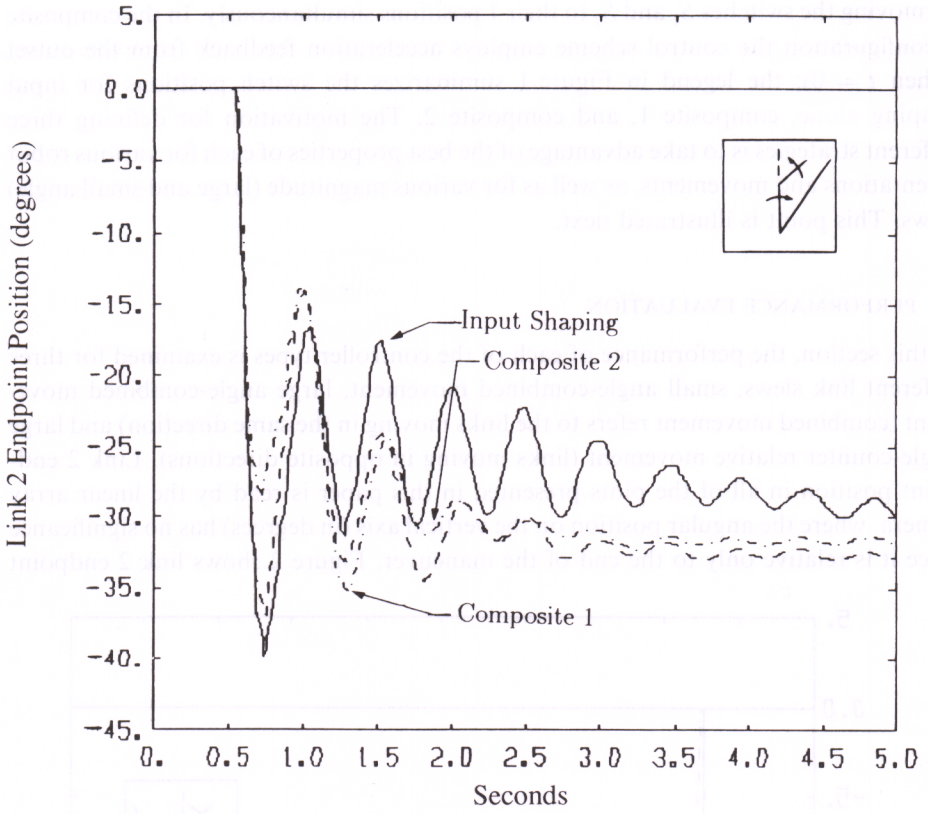

Fig. 4. Link 2 endpoint position for large-counter relative link slews.

when the links are slewed approximately 25°. It can be noticed that the input shaping configuration exhibits less overshoot and faster settling time than the other configurations. The modal dampings and frequencies used for this and all other experiments in this section are 0.11 and 1.06 Hz for link 1 and 0.065 and 2.32 Hz for link 2, and $A_1 = 0.35$ V and $a_2 = 3.5$ V. Moreover, the shaft position and feedback acceleration gains were set to the following values $K_{p1} = 0.0025$, $K_{a1} = -0.2$, $K_{p2} = 0.01$ and $K_{a2} = -0.3$. These controller input parameters, hereafter referred to as 'nominal' modal frequencies, dampings and amplitudes, were experimentally tuned to obtain the best steady-state response over 'all' possible slews.

Figure 3 shows that for a large angle maneuver ($\theta_1 = 45°$, $\theta_2 = 90°$) the composite 1 configuration, although having large undershoot, is able to control the residual vibrations better than the other configurations, since the composite 2 response results in a steady-state position error. Lastly, Figure 4 shows that for counter relative link slews, i.e. links moving in opposite direction ($\theta_1 = 45°$, $\theta_2 = -60°$), the composite 2 configuration dampens the link vibrations faster than the other configurations.

It is evident from these experimental results that no controller type performs better than the others for 'all' possible links slews. For this reason, a logical next step to

follow is to use a supervisory control scheme that determines, among other things, which controller to use depending on the desired link endpoint positions. The development of such a control strategy which incorporates fuzzy logic is discussed next.

4. Supervisory Control Framework

The three subsystems that make up the supervisory control strategy are shown in Figure 5. This strategy constitutes the high level, while the input shaping and composite controllers presented in the last section represent the low level of the hierarchical control structure proposed in this paper. It is evident from the figure that both reference angles constitute the inputs to the supervisory controller. The output of Subsystem A is an integer that selects the low level controller type to be executed (see Figure 1). The operations that this subsystem perform can be summarized as follows:

$$\text{controller type } i = \begin{cases} 1 & \text{if } 0 \leqslant \theta_{\text{ref}1} < 25^\circ \text{ and } 0 \leqslant \theta_{\text{ref}2} < 25^\circ \\ 1 & \text{if } -25^\circ < \theta_{\text{ref}1} < 0 \text{ and } -25^\circ < \theta_{\text{ref}2} < 0 \\ 3 & \text{if } \theta_{\text{ref}1}\theta_{\text{ref}2} < 0 \\ 2 & \text{otherwise} \end{cases} \tag{16}$$

Hence the controller selector is a simple rule-based system which chooses the best controller to achieve the particular commanded $\theta_{\text{ref}1}$ and $\theta_{\text{ref}2}$. The rules in the controller selector, which are described by Equation (16), incorporate the information obtained from the experiments in Section 3. Specifically, for combined link movements under 25° the input shaping configuration (controller type 1) cancels the

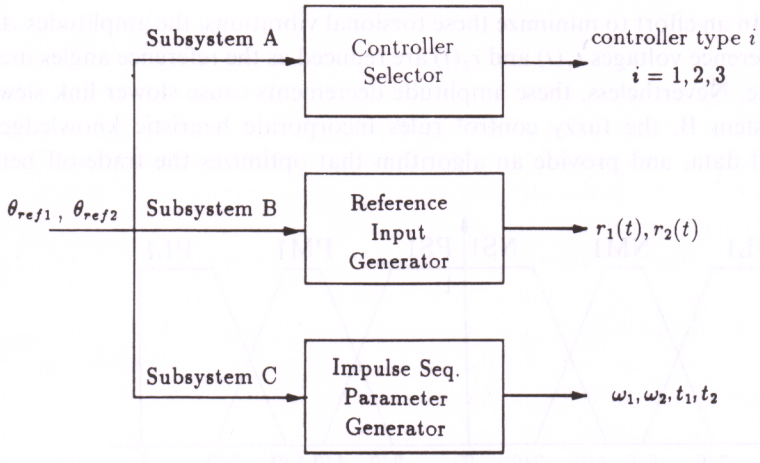

Fig. 5. Supervisory control subsystems.

link endpoint vibrations faster than the other two controllers (see Figure 2). Conversely, different experiments, such as those shown in Figure 3, illustrate that when both links move over 25° in the same direction, the composite 1 configuration (controller type 2) best produces steady endpoint position of the links. Lastly, experiments also show that for any maneuver commanding the links to move in opposite directions the composite 2 configuration (controller type 3) is able to minimize the residual vibrations faster than the other configurations.

Subsystems B and C consist of the four blocks proposed by Lee in [14], namely a fuzzification interface, a decision making logic, a defuzzification interface and a knowledge data base; however, here the fuzzification is performed *a priori*. The universes of discourse for θ_{ref1} and θ_{ref2} are defined on the interval $[-90°, 90°]$ for both subsystems, B and C. For convenience, we normalize these universes of discourse. Consequently, the normalized universes of discourse for the normalized input variables $\hat{\theta}_1$ and $\hat{\theta}_2$ are defined on the interval $[-1, 1]$. Figure 6 shows the fuzzy sets and their membership functions for the normalized input variable $\hat{\theta}_1$. Identical membership functions are used for $\hat{\theta}_2$. The acronyms NL1, NM1 and NS1 represent the fuzzy labels associated with the three leftmost fuzzy sets and represent a negative large, negative medium and negative small angle $\hat{\theta}_1$. In a similar manner the prefix P is used to denote the positive angles. Moreover, the membership functions of these sets will be denoted by μ_{NL1}, μ_{NM1}, μ_{NS1}, etc. Similar notation is used for the membership functions for $\hat{\theta}_2$. The reason for choosing such membership function shapes is justified by the experimental results; this point is discussed further in the next section.

Again, a closer look at Figure 5 shows that Subsystem B outputs the reference input profiles $r_1(t)$ and $r_2(t)$ (amplitudes A_1, A_2 and time durations t_{01}, t_{02}) to be convolved with the impulse sequences that shape the actuator inputs (see Figure 1). Experiments show that as the angle between the links increases, the out of plane (torsional) vibrations also increase. These negative effects are further enhanced by fast link maneuvers. In an effort to minimize these torsional vibrations, the amplitudes A_1 and A_2 of the reference voltages $r_1(t)$ and $r_2(t)$ are reduced as the reference angles increase in magnitude. Nevertheless, these amplitude decrements cause slower link slews.

In Subsystem B, the fuzzy control rules incorporate heuristic knowledge and experimental data, and provide an algorithm that optimizes the trade-off between

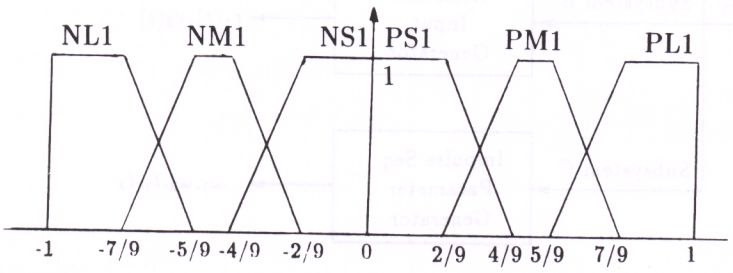

Fig. 6. Subsystems B and C fuzzy partition of $\hat{\theta}_1$.

Table I. Supervisory control rules for subsystem B.

	Condition		Output			Condition		Output	
rule	$\hat{\theta}_1$	$\hat{\theta}_2$	$\hat{V}_1^i$	$\hat{V}_2^i$	rule	$\hat{\theta}_1$	$\hat{\theta}_2$	$\hat{V}_1^i$	$\hat{V}_2^i$
R_1^B	PL1	PL2	0.3 V	3.0 V	R_{19}^B	PL1	NL2	0.3 V	−3.0 V
R_2^B	PM1	PL2	0.35 V	3.0 V	R_{20}^B	PM1	NL2	0.35 V	−3.0 V
R_3^B	PS1	PL2	0.4 V	3.0 V	R_{21}^B	PS1	NL2	0.4 V	−3.0 V
R_4^B	PL1	PM2	0.3 V	3.5 V	R_{22}^B	PL1	NM2	0.3 V	−3.5 V
R_5^B	PM1	PM2	0.35 V	3.5 V	R_{23}^B	PM1	NM2	0.35 V	−3.5 V
R_6^B	PS1	PM2	0.4 V	3.5 V	R_{24}^B	PS1	NM2	0.4 V	−3.5 V
R_7^B	PL1	PS2	0.3 V	4.0 V	R_{25}^B	PL1	NS2	0.3 V	−4.0 V
R_8^B	PM1	PS2	0.35 V	4.0 V	R_{26}^B	PM1	NS2	0.35 V	−4.0 V
R_9^B	PS1	PS2	0.4 V	4.0 V	R_{27}^B	PS1	NS2	0.4 V	−4.0 V
R_{10}^B	NL1	NL2	−0.3 V	−3.0 V	R_{28}^B	NL1	PL2	−0.3 V	3.0 V
R_{11}^B	NM1	NL2	−0.35 V	−3.0 V	R_{29}^B	NM1	PL2	−0.35 V	3.0 V
R_{12}^B	NS1	NL2	−0.4 V	−3.0 V	R_{30}^B	NS1	PL2	−0.4 V	3.0 V
R_{13}^B	NL1	NM2	−0.3 V	−3.5 V	R_{31}^B	NL1	PM2	−0.3 V	3.5 V
R_{14}^B	NM1	NM2	−0.35 V	−3.5 V	R_{32}^B	NM1	PM2	−0.35 V	3.5 V
R_{15}^B	NS1	NM2	−0.4 V	−3.5 V	R_{33}^B	NS1	PM2	−0.4 V	3.5 V
R_{16}^B	NL1	NS2	−0.3 V	−4.0 V	R_{34}^B	NL1	PS2	−0.3 V	4.0 V
R_{17}^B	NM1	NS2	−0.35 V	−4.0 V	R_{35}^B	NM1	PS2	−0.35 V	4.0 V
R_{18}^B	NS1	NS2	−0.4 V	−4.0 V	R_{36}^B	NS1	PS2	−0.4 V	4.0 V

speed of link maneuvers and reduction of torsional vibrations. This is obtained by gradually adjusting the reference voltage amplitudes depending not only on the angle between the links but also on their final endpoint positions. Consequently, this approach presents an alternative to the cumbersome derivation of the equations that relate the input voltage to the torsional vibrations of the manipulator. Table I depicts the conditional rules (denoted by R_i^B) developed in the decision making logic of Subsystem B to minimize these undesirable vibrations. The experimentally determined values of the control actions associated with rule R_i^B are $\hat{V}_1^i$ and $\hat{V}_2^i$. The number of fuzzy sets in a fuzzy input space determines the maximum number of control rules that can be constructed, but as indicated in [15], the performance of the conditional rules can be improved by using the maximum number possible. It is for this reason that all the possible conditional rules (36) are used here.

It is clear from Table I that this is a multi-input, multi-output subsystem, therefore the control rules all have a form similar to that of rule 17, or

$$\text{If } \hat{\theta}_1 \text{ is NM1} \quad \text{and} \quad \hat{\theta}_2 \text{ is NS2} \quad \text{then } \hat{V}_1^{17} = -0.35\,\text{V} \quad \text{and} \quad \hat{V}_2^{17} = -4.0\,\text{V}.$$

This control rule can be decomposed into

$$\text{If } \hat{\theta}_1 \text{ is NM1} \quad \text{and} \quad \hat{\theta}_2 \text{ is NS2} \quad \text{then } \hat{V}_1^{17} = -0.35\,\text{V},$$

$$\text{if } \hat{\theta}_1 \text{ is NM1} \quad \text{and} \quad \hat{\theta}_2 \text{ is NS2} \quad \text{then } \hat{V}_2^{17} = -4.0\,\text{V}.$$

Since both decomposed rules are conditioned by the same input, their premises have the same degree of fulfillment which we denote with $\mu_{R_i^B}$. The degree of fulfillment of the premise of each rule represents the intersection or union of the fuzzy sets, as

defined in [16]; hence, the degree of fulfillment of the premise of R_{17}^B is calculated as

$$\mu_{R_{17}^B} = \min\left(\mu_{NM1}(\hat{\theta}_1), \mu_{NS2}(\hat{\theta}_2)\right). \tag{17}$$

Moreover, computational savings can be obtained since only the degrees of fulfillment of one input variable are needed to calculate the control value of both fuzzy input variables $\hat{\theta}_1$ and $\hat{\theta}_2$; this is illustrated next.

Following the method proposed in [17] the 'crisp' control action is found by combining the action specified by each rule in proportion to the associated degree of fulfillment of each rule. Using the aforementioned method, the reference input amplitudes A_1 and A_2 that try to minimize the torsional vibrations are calculated in the manner

$$A_1 = \frac{\sum_{i=1}^{36} \hat{V}_1^i \mu_{R_i^B}}{\sum_{i=1}^{36} \mu_{R_i^B}}, \tag{18}$$

$$A_2 = \frac{\sum_{i=1}^{36} \hat{V}_2^i \mu_{R_i^B}}{\sum_{i=1}^{36} \mu_{R_i^B}}. \tag{19}$$

Since each rule degree of fulfillment has the same value while determining A_1 and A_2, the same formula can be used to calculate these amplitudes by simply varying the actions to be taken. To illustrate how the crisp control actions are determined, consider the case where $\hat{\theta}_1 = -\frac{1}{2}$ and $\hat{\theta}_2 = -\frac{1}{4}$. It can be seen from Figure 6 that for $\hat{\theta}_1 = -\frac{1}{2}$, $\mu_{NM1}(-\frac{1}{2}) = 1$ while the values of the other membership functions are zero. On the other hand, even though $\hat{\theta}_2$ belongs strongly to set NS2, it also belongs to NM2 as it is shown by the value of the membership functions $\mu_{NS2}(-\frac{1}{4}) = \frac{7}{8}$ and $\mu_{NM2}(-\frac{1}{4}) = \frac{1}{8}$. From Table I, we see that only the premises R_{14}^B and R_{17}^B have nonzero degrees of fulfillments as defined by Equation (17), and they take on values $\frac{1}{8}$ and $\frac{7}{8}$, respectively. Finally as in [17] the crisp reference amplitude values are given by

$$A_1 = \frac{(-0.35)\frac{1}{8} + (-0.35)\frac{7}{8}}{\frac{1}{8} + \frac{7}{8}} = -0.35\,\text{V},$$

$$A_2 = \frac{(-3.5)\frac{1}{8} + (-4.0)\frac{7}{8}}{\frac{1}{8} + \frac{7}{8}} = -3.9375\,\text{V}.$$

To completely determine the actuator reference inputs, the time of duration of the constant voltages also needs to be calculated. The procedure followed here to determine t_{01} and t_{02} is to use linear interpolation from experimentally determined data tables that specify the duration times for link slews between 0° and 90° in steps of 10° when 0.3 V, 0.35 V and 0.4 V are applied to actuator 1, and 3.0 V, 3.5 V and 4.0 V to actuator 2. This table is presented and described in [11].

Next we will specify the fuzzy supervisory algorithm used in Subsystem C. As indicated earlier, the modal frequencies of each link vary as the angle between the links vary [10]. Subsystem C attempts to adjust the time of application of the impulses

Table II. Supervisory control rules for subsystem C.

	Condition		Output	
rule	$\lvert\hat{\theta}_1\rvert$	$\lvert\hat{\theta}_2\rvert$	$\hat{\Omega}_1^j$	$\hat{\Omega}_2^j$
R_1^C	PL1	PL2	1.042 Hz	2.35 Hz
R_2^C	PM1	PL2	1.031 Hz	2.35 Hz
R_3^C	PS1	PL2	1.02 Hz	2.35 Hz
R_4^C	PL1	PM2	1.042 Hz	2.304 Hz
R_5^C	PM1	PM2	1.031 Hz	2.304 Hz
R_6^C	PS1	PM2	1.02 Hz	2.304 Hz
R_7^C	PL1	PS2	1.042 Hz	2.127 Hz
R_8^C	PM1	PS2	1.031 Hz	2.127 Hz
R_9^C	PS1	PS2	1.02 Hz	2.127 Hz

by varying ω (Equation (7)) as the input angles $\theta_{\text{ref}1}$ and $\theta_{\text{ref}2}$ vary. The difficulty of implementing this controller lies in the fact that the manipulator dynamics are nonlinear and time varying; therefore, determining the modal frequencies of the links analytically is a difficult problem in itself. Moreover, these frequencies vary with respect to the link configurations. Here the modal frequencies corresponding to small, medium and large links slews were determined experimentally.

Fuzzification for $\theta_{\text{ref}1}$ and $\theta_{\text{ref}2}$ for this subsystem is the same as Subsystem B. The control rules follow the same 'conditions' as the ones shown in Table I. However, it was determined experimentally that the modal frequencies do not vary with respect to the direction of the slew, therefore the control action is the same despite the signs of the reference angles. This fact allows the 36 possible supervisory control rules to be expressed in the form shown in Table II. Again, the experimentally determined values $\hat{\Omega}_j^i$ associated with each rule are also shown in the table.

Lastly, the defuzzification interface for this subsystem is also performed in the same manner as for Subsystem B; thus, the modal frequencies used to calculate the spacing between impulses for the input shaping schemes are determined by

$$\omega_j = \frac{\sum_{i=1}^{9} \hat{\Omega}_j^i \mu_{R_i^C}}{\sum_{i=1}^{9} \mu_{R_i^C}}, \quad j = 1, 2. \tag{20}$$

In summary, we provide a brief description of the functional operation of the fuzzy supervisor. The angles $\theta_{\text{ref}1}$ and $\theta_{\text{ref}2}$ are the inputs to the three subsystems. The controller selector chooses one of the three controller types discussed in the previous section that best minimizes the endpoint vibrations in the links depending on the value of the reference angles. The reference input generator determines the constant amplitude and time of duration of $r_1(t)$ and $r_2(t)$ that are used as inputs for the low level controllers, and that attempt to minimize the torsional vibrations in the links. Lastly, the impulse sequence parameter generator adjusts the modal frequencies that determine the spacing, as given by Equation (7), between the impulses in the impulse sequence (Equation (13)) that minimize the link bending vibrations by shaping the actuator reference voltages.

5. Experimental Results

The experimental results included in this section serve two purposes. First, they show the effects that variations in the link modal frequencies ω_1 and ω_2 have on the link endpoint position control. Consequently, a different set of experimental results are included to illustrate the success of the hierarchical control strategy in effectively achieving accurate and steady link endpoint position in both combined and counter relative maneuvers. For illustrative purposes, the results of the latter controller are compared to those using the 'nominal' control input parameters described in Section 3.

Before we begin with these discussions, however, it is important to note that experimental results also show that the torsional vibrations are minimized as the amplitudes of the reference voltages are decreased, i.e. the conditional rules of Subsystem B were successful in calculating reference voltages that minimize the out-of-plane vibrations. However, because the recording device is a *linear* array camera motions in any vertical plane cannot be recorded, and are not shown.

The link 2 end-point position plots shown in Figures 7 and 8 depict the performance of the input shaping (controller type 1) scheme as the modal frequencies ω_1 and ω_2

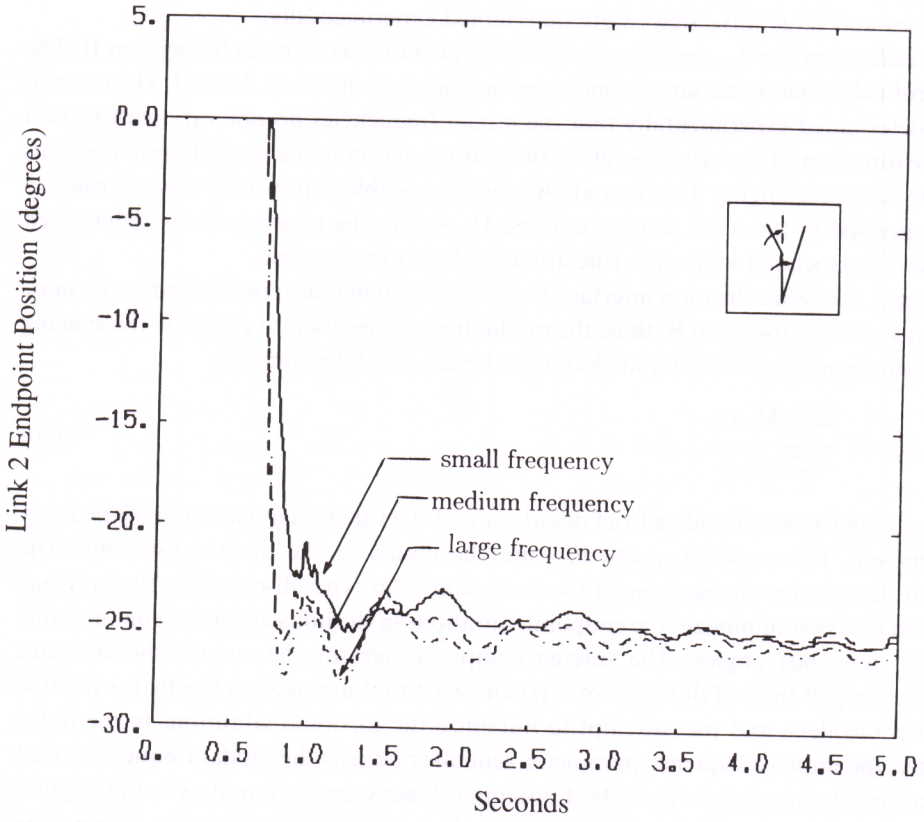

Fig. 7. Small angle slews with adjusted modal frequencies.

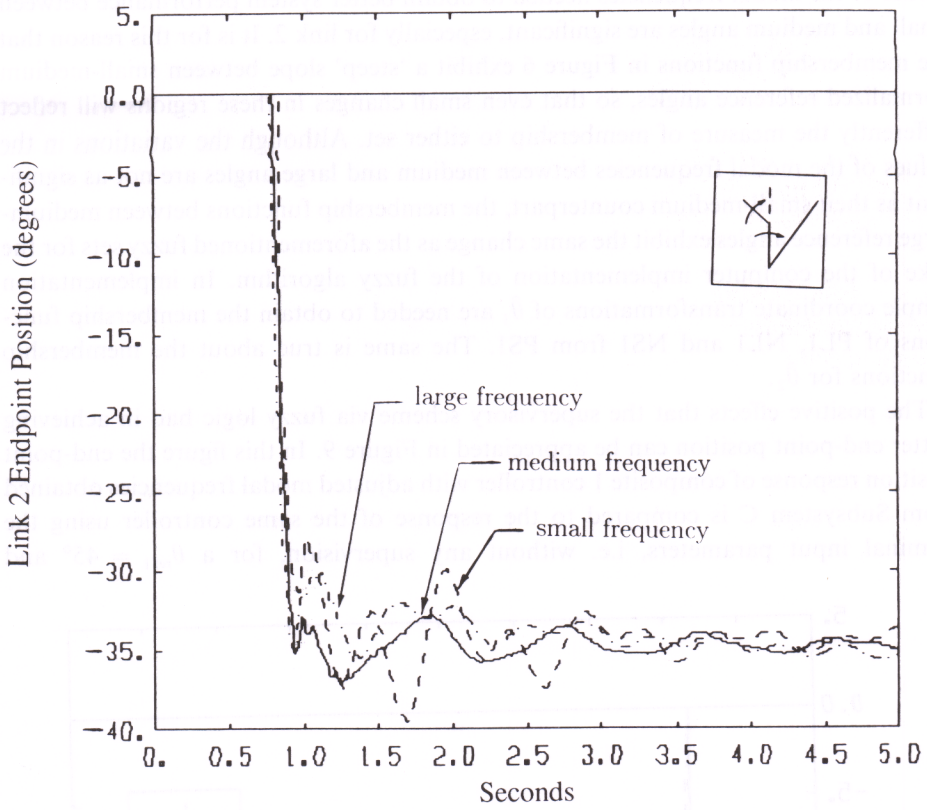

Fig. 8. Medium angle slews with adjusted modal frequencies.

are adjusted to minimize residual vibrations depending on the reference angles. Similar experiments were conducted to determine the control values for each supervisory control rule in Table II. These control actions indicate that as the reference angles increase, the modal frequencies adjusted to minimize the link structural vibrations also increase. Figure 7 shows that for small angles ($\theta_1 = 20°$, $\theta_2 = 20°$) the response shaped for small modal frequencies exhibits less residual vibrations than the other two responses shaped for medium and large angles. Conversely, Figure 8 shows that for medium angles (45°, 45°) the response shaped for medium frequencies demonstrates less end-point oscillations than the other two responses. Lastly, experiments also showed that for large angle slews the response shaped for large angles exhibits less residual vibrations than the other two responses. Note that although Subsystem A specifies that the low level controller used in these experiments, namely controller type I, would not be selected for slews over 25°, results are intended to illustrate the improvements that can be obtained by adjusting the link modal frequencies in the other two controller types that are also based on the input shaping method.

Next we will discuss the reason for choosing the membership function shapes as shown in Figure 6. Experimentally obtained data showed that the differences in the

values of the modal frequencies needed to obtain better system performance between small and medium angles are significant, especially for link 2. It is for this reason that the membership functions in Figure 6 exhibit a 'steep' slope between small-medium normalized reference angles, so that even small changes in these regions will reflect differently the measure of membership to either set. Although the variations in the values of the modal frequencies between medium and large angles are not as significant as their small-medium counterpart, the membership functions between medium-large reference angles exhibit the same change as the aforementioned fuzzy sets for the sake of the computer implementation of the fuzzy algorithm. In implementation simple coordinate transformations of $\hat{\theta}_1$ are needed to obtain the membership functions of PL1, NL1 and NS1 from PS1. The same is true about the membership functions for $\hat{\theta}_2$.

The positive effects that the supervisory scheme via fuzzy logic had in achieving better end-point position can be appreciated in Figure 9. In this figure the end-point position response of composite 1 controller with adjusted modal frequencies obtained from Subsystem C is compared to the response of the same controller using the nominal input parameters, i.e. without any supervision, for a $\theta_{\text{ref}1} = 45°$ and

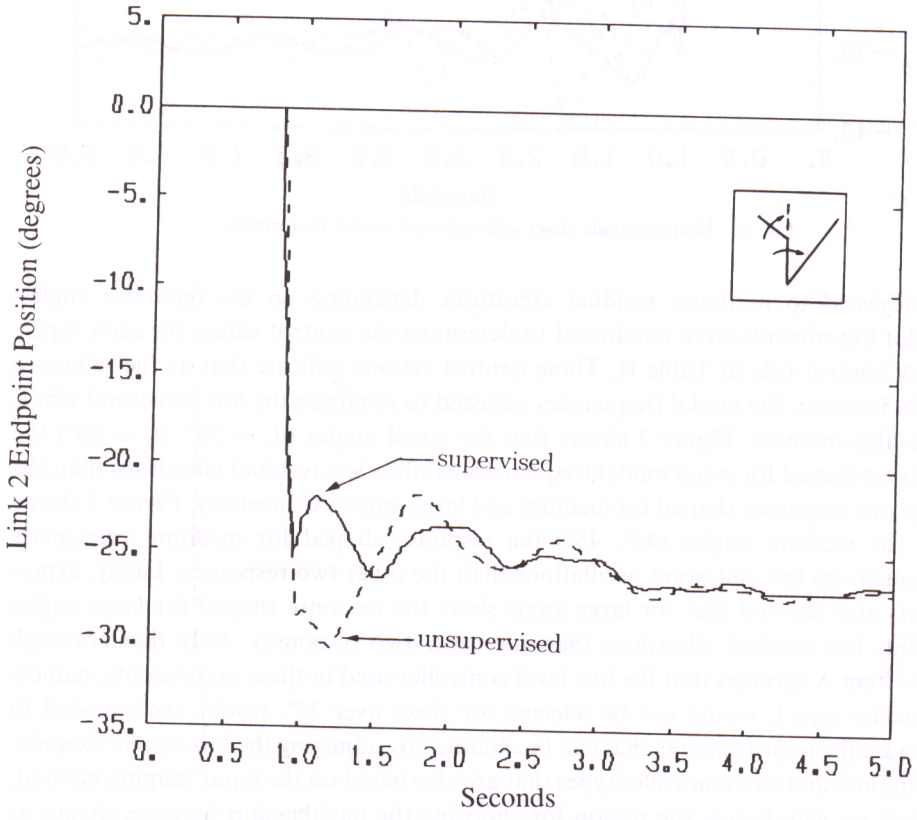

Fig. 9. Combined movement end-point position for supervised and unsupervised systems.

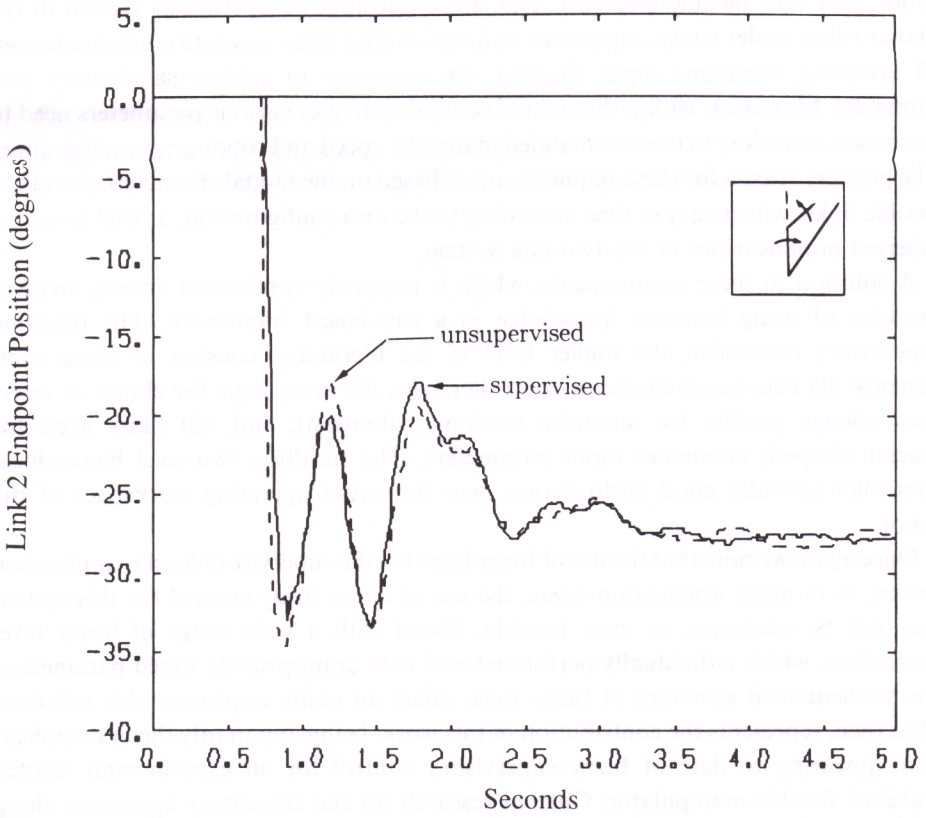

Fig. 10. Counter movement end-point position for supervised and unsupervised systems.

$\theta_{\text{ref}2} = 60°$ slew. Clearly, the over(under)shoot and settling time characteristics of the supervised system are better than the unsupervised system. Similar improvements were observed for other commanded slews when the composite 1 controller was used.

Figure 10 shows that for a counter-relative slew (45°, −60°) the composite 2 controller with adjusted frequencies exhibits better steady endpoint position response than the one using the nominal input parameters. In general, for counter-relative movements the supervisor allowed the composite 2 controller to obtain a steadier endpoint position than when no modal frequency adjustments were made, regardless of the magnitude of the commanded counter-relative slew.

From these experiments then, we can conclude that by using the supervisory controller a faster and more steady endpoint position is obtained for 'any' possible commanded slew on the interval [−90°, 90°]. In addition, whenever the supervisor selects the composite 1 controller better system over(under)shoot characteristics are obtained.

6. Conclusions

In this paper a two level hierarchical control strategy was presented to improve performance of existing techniques for endpoint position control of a two-link

robot with very flexible members. For the wide range of operations typical in the planar robot under study, experience had shown that three separate control schemes, all involving command input shaping, are necessary to achieve satisfactory performance. Moreover, within these three control strategies various parameters need to be chosen according to the commanded maneuver speed and robot arm configuration. The primary reason for these requirements is based on the modal characteristics of the flexible links, which vary in time according to the arm configuration, as well as on the inherent nonlinearities of the two-link system.

A solution to these requirements, which is primarily application driven, involves the idea of using heuristic knowledge in a rule-based framework. The resulting supervisory controller, the higher level in the hierarchy, consists of three components: (1) rule-based choice of controller type; (2) fuzzy logic for choice of reference voltage profiles (to minimize torsional vibration); and, (3) fuzzy logic for crucial (shaped) command input parameters. The resulting two-level hierarchical controller provides good performance over the entire operating workspace of the robot.

Once again we note that the use of fuzzy logic for the supervisory level is application driven; as in many application areas, the use of *direct* fuzzy control for this system may not be necessary, or even feasible. Faced with a wide range of lower level controllers, which individually performed well with appropriately tuned parameters, the mathematical structure of fuzzy logic offers an easily implementable solution. This, then, represents the contribution of this work, being apparently the first application appearing to date of fuzzy supervisory control for an experimental testbed multilink flexible manipulator. Current research for the laboratory apparatus along these lines involves utilizing fuzzy logic for an inner feedback loop in the rigid body motion control, and in payload identification.

References

1. Antsaklis, P.J., Passino, K.M. and Wang, S.J., Towards intelligent autonomous control systems: Architecture and fundamental issues, *J. Intelligent and Robotic Systems* **1**, 315–342 (1989).
2. Antsaklis, P.J., Passino, K.M. and Wang, S.J., An introduction to autonomous control systems, *IEEE Control Systems* **11**(4), 5–13 (1991).
3. Yurkovich, S. and Pacheco, F.E., On controller tuning for a flexible-link manipulator with varying payload, *J. Robotic Systems* **6**, 233–254 (June 1989).
4. Yurkovich, S. and Tzes, A.P., Experiments in the identification and control of flexible-link manipulators, *IEEE Control Systems* **10**, 41–47 (February 1990).
5. Rovner, D.M. and Franklin, G.F., Experiments in load-adaptive control of a very flexible one-link manipulator, *Automatica* **24**, 541–548 (July 1988).
6. Oakley, C. and Cannon, R., Endpoint control of a two link manipulator with a very flexible forearm: issues and experiments, in *Proc. American Control Conference*, pp. 1381–1388, Pittsburgh PA (May 1989).
7. Singer, N. and Seering, W., Preshaping command inputs to reduce system vibrations, Technical Report A.I. Memo No. 1027, MIT Artificial Intelligence Laboratory (1988).
8. Tzes, A., Englehart, M. and Yurkovich, S., Input preshaping with frequency domain information for flexible link manipulator control, in *Proc. AIAA Guidance, Navigation and Control Conference*, Boston MA (August 1989).

9. Hillsley, K. and Yurkovich, S., Vibration control of a two-link flexible robot arm, in *Proc. IEEE Int. Conference on Robotics and Automation* (April 1991).
10. Yurkovich, S., Tzes, A. and Hillsley, K., Controlling coupled flexible links rotating in the horizontal plane, in *Proc. American Control Conference*, San Diego CA (May 1990).
11. Garcia-Benitez, E., Conventional and rule-based control design for a two-link flexible manipulator, *MS thesis*, The Ohio State University, Department of Electrical Engineering (1991).
12. Yurkovich, S., Hillsley, K.L. and Tzes, A.P., Identification and control for a manipulator with two flexible links, in *Proc. IEEE Conference on Decision and Control*, pp. 1995–2000, Honolulu, Hawaii (December 1990).
13. Tzes, A. and Yurkovich, S., A frequency domain identification scheme for flexible structure control, *Trans. ASME, J. Dynamic Systems, Measurement and Control* **111**, 427–434 (September 1990).
14. Lee, C.C., Fuzzy logic in control systems: fuzzy logic controller – Part I, *IEEE Trans. Systems Man Cybernet.* **20**, 404–418 (March/April 1990).
15. Sugeno, M., An introductory survey of fuzzy control, *Information Sciences* **36** 59–83 (1985).
16. Zadeh, L.A., Outline of a new approach to the analysis of complex systems and decision processes, *IEEE Trans. Systems Man Cybernet.* **3**, 28–44 (1973).
17. Bernard, J., Use of a rule-based system for process control, *IEEE Control Systems* **8**, 3–13 (October 1988).